



INFLUENCE OF THERMODYNAMIC PROCESS PARAMETERS ON THE ACOUSTIC PROPERTIES OF ELECTRIC REFRIGERANT SCROLL COMPRESSORS

Lukas Saur^{1*}

Stefan Becker¹

¹ Institute of Fluid Mechanics, Friedrich-Alexander University Erlangen-Nuremberg, Germany

ABSTRACT

With the ongoing electrification of vehicles, the acoustic properties of the vehicle's interior are increasingly affected by auxiliary units. In electric vehicles, the battery and the electric motors must be cooled in addition to the passenger cell. Therefore, larger A/C compressors are needed, which increase sound radiation and vibration excitation. The compressor is the central sound source in the refrigeration circuit, on the one hand through direct airborne sound radiation, on the other hand it causes acoustic excitation of other refrigeration circuit components via pressure pulsations and vibration transmission. To characterize the acoustic properties of refrigerant scroll compressors, a test rig was developed that allows an isolated observation of the acoustic properties of refrigerant compressors in an anechoic chamber. This paper investigates the influence of thermodynamic process variables on compressor acoustics and shows that increasing speed and compression ratio lead to greater sound radiation. The sound spectra of fluid, structure and airborne noise are dominated by speed-dependent, tonal components. The findings provide insights into the physical relationship between thermodynamic and acoustic parameters and enable the identification of a low noise operating range.

Keywords: *compressor acoustics, scroll compressor, nvh, refrigerant cycle, vibroacoustics*

*Corresponding author: lukas.saur@fau.de.

Copyright: ©2023 Saur et al. This is an open-access article distributed under the terms of the Creative Commons Attribution 3.0 Unported License, which permits unrestricted use, distribution, and reproduction in any medium, provided the original author and source are credited.

1. INTRODUCTION

In March this year, the EU Parliament decided that from 2035 onwards, newly registered passenger cars will no longer be allowed to emit CO₂ in order to further accelerate the electrification of the vehicle market [1]. In battery-electric vehicles, the thermal management system plays a key role, high efficiency and pleasant acoustics are crucial. The efficiency has a direct influence on the achievable range, while at the same time increased requirements apply to the acoustics, due to the elimination of the masking noise of the combustion engine [2,3]. One of the dominant sound sources in the thermal management system is the refrigerant compressor [4].

Mechanical, electromagnetic and fluid dynamic excitations occur in scroll compressors. The dynamic excitations are mainly transmitted to the housing, as it is a hermetically sealed unit, and result in vibrations of the housing system [5]. Lee et al. [6] and Miao et al. [7] showed that the airborne sound radiation correlates with the vibrations of the compressor and that vibrational resonances of the casing can lead to a strong increase of the radiated airborne sound. In the investigations of Haeussler et al. [8], sound radiation of an electric scroll compressor is proportional to the rotation speed. Yanagisawa et al. [9] were able to establish a connection between the suction pressure and the sound radiation, as well as to prove the excitation of vibration resonances of the compressor shaft by high pressure pulsations. Currently, research on the acoustics of scroll compressors mainly involves numerical simulation methods for calculating sound radiation and optimising individual compressor components for sound reduction. However, there are only a few studies on the influence of thermodynamic boundary conditions on compressor acoustics.



The aim of this paper is to determine the influence of various thermodynamic process variables on the fluid, body and airborne sound of an electric scroll compressor. In a first step, a suitable test rig was developed on which the compressor acoustics can be measured under precisely adjustable thermodynamic boundary conditions. Subsequently, the influence of rotation speed, compression ratio, suction and high pressure on the acoustic properties of the scroll compressor was investigated.

2. EXPERIMENTAL SETUP

The investigations were carried out on a refrigerant compressor acoustic test rig set up for this purpose. To set precisely defined thermodynamic operating points, the compressor is integrated into a refrigeration circuit in which the heat flows at the heat exchangers and the throttling effect of the expansion valve are controlled accordingly. The acoustic behaviour of the scroll compressor was characterised with the help of pressure pulsation sensors, acceleration sensors and microphones inside an anechoic chamber.

2.1 Refrigeration cycle

In order to be able to fully characterise the acoustics of the refrigerant compressor, a refrigeration cycle is available that allows the compressor to be run in the entire operating range. The environmentally friendly chemical refrigerant 2,3,3,3-tetrafluoropropene (R1234yf), which is common in the automotive sector, is used. Figure 1 shows the schematic test rig setup.

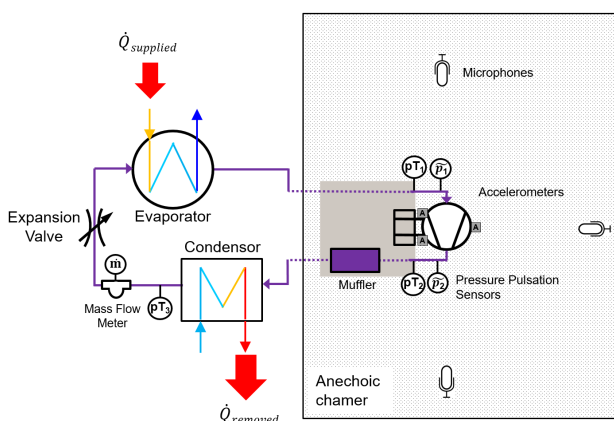


Figure 1. Schematic test rig design

The compressed refrigerant flows into a water-cooled condenser and is completely liquefied. The liquid refrigerant is expanded with the aid of the expansion valve. Pressure difference and refrigerant mass flow can be adjusted via the electronically adjustable throttle effect of the valve. In the following refrigerant-water heat exchanger, the refrigerant is evaporated under heat supply and then sucked in again by the compressor. Pressure and temperature (pT) sensors before and after the compressor as well as after the condenser capture the relevant data for determining the operating point. A Coriolis mass flow meter measures the refrigerant mass flow.

Only the compressor and a flow silencer are placed inside the anechoic chamber, all other test stand components are located outside to avoid disturbing noise. The flow silencer reduces pressure pulsations on the high-pressure side in order to reduce the vibro-acoustic excitation of the remaining refrigeration cycle components. The flow silencer is covered with acoustically dampening foam to minimise interfering noise. Flexible refrigerant hoses are used to decouple the compressor and the rest of the test stand components in terms of vibration. Cables and refrigerant hoses are routed inside the anechoic chamber through an acoustically insulated passage.

2.2 Acoustic measurement setup

The sensors used for acoustic characterisation and their positions are shown in Fig. 2. The compressor is firmly bolted to a 600 kg concrete cube via a solid steel bracket in order to minimise influences of the attachment on compressor vibrations. Triaxial acceleration sensors are mounted on the housing at the three bolting points to measure the compressor vibrations (3B-1, 3B-2, 3B-3). As a further acoustic excitation variable, the pressure pulsations at the compressor inlet (\tilde{p}_1) and at the compressor outlet (\tilde{p}_2) are recorded. The sound radiation of the scroll compressor is measured under free-field conditions in an anechoic chamber in the 5 free radiation directions using free-field microphones (see Fig. 3).

3. ACOUSTICS OF THE REFERENCE OPERATING POINT

In this chapter, the spectral curves of the investigated acoustic variables of the reference measurement at a medium compressor speed of 5000 rpm and a medium compression ratio of 7 are evaluated.

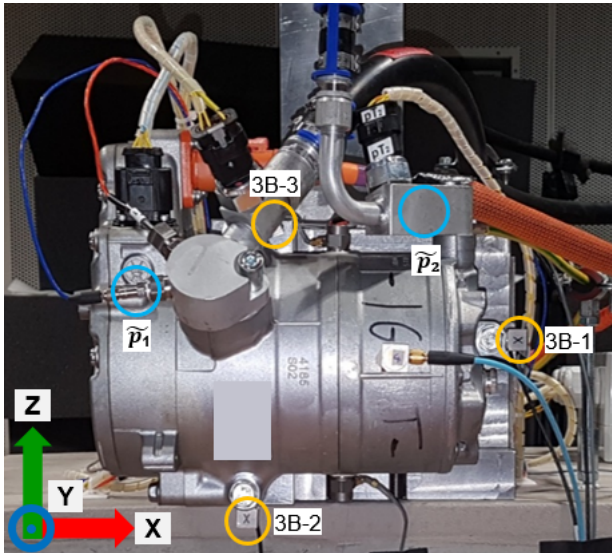


Figure 2. Accelerometers (yellow) and pressure pulsation sensors (blue) on the compressor

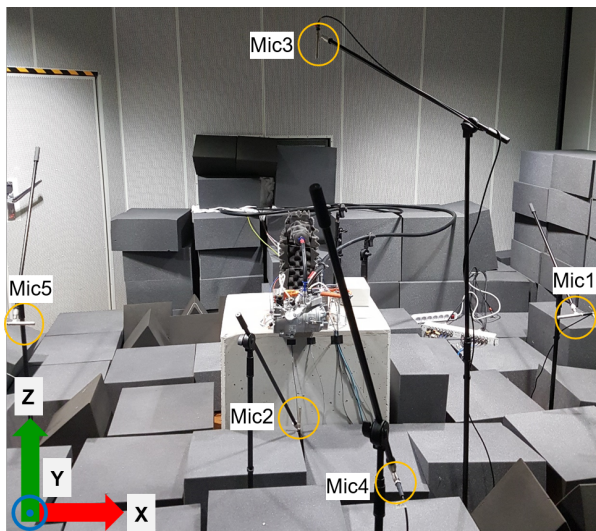


Figure 3. Microphones in the anechoic chamber

3.1 Fluid sound

The cyclic compression principle of the scroll compressor results in a fluctuating pressure curve. To illustrate the operating principle of scroll compressors, Fig. 4 shows the pressure distribution in the compression chamber of a scroll compressor for different crankshaft angles.

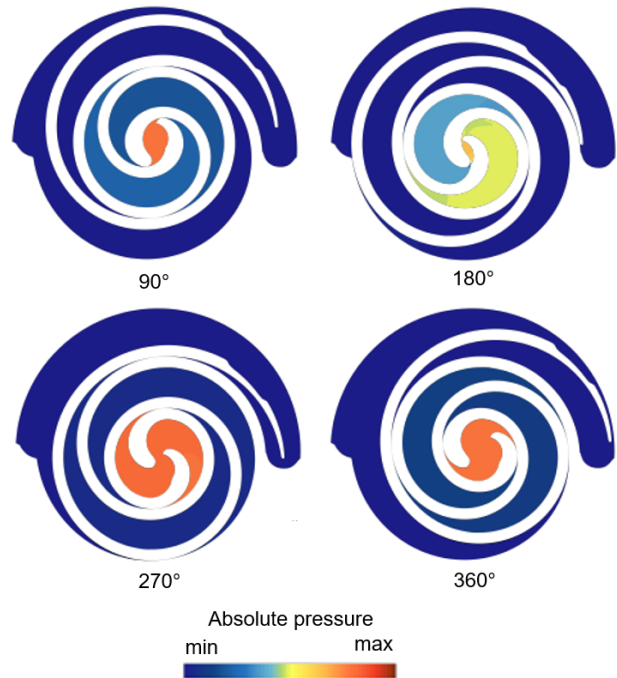


Figure 4. Pressure distribution in the compression chamber at different crankshaft angles

These pressure fluctuations lead to the excitation of vibrations and the radiation of airborne sound in all components of the refrigeration cycle and are therefore an important acoustic parameter. The spectrum of the suction pressure pulsations (see Fig. 5) shows that, the first two orders of the rotational frequency are dominant, due to the design of the scroll compressor. With each revolution of the compressor screw, the two outer compression chambers open once (see Fig. 4) and gaseous refrigerant is sucked in on the low-pressure side. The frequency of the other peaks in the sound pressure spectrum are also integer multiples of the rotation frequency. These higher-harmonic pressure pulsations are caused by flow reflections at bends and cross-sectional jumps in the refrigeration cycle. The amplitude of the suction pressure pulsations drops at approx. 20 dB per decade for frequencies greater than 400 Hz.

As Fig. 6 shows, pulsations of the 1st order are dominant at the compressor outlet, since the check valve at the discharge bore opens once per revolution as soon as the pressure in the inner compression chamber is greater than the pressure in the downstream high-pressure line. The re-

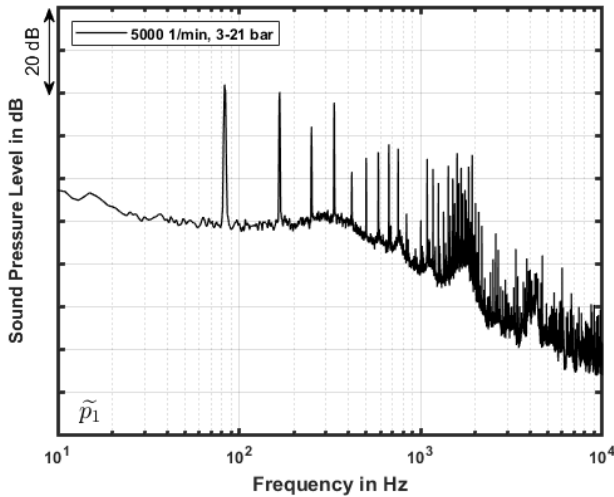


Figure 5. Suction pressure pulsations

duction of the 2nd to 4th order pressure pulsations in the frequency range of 150-350 Hz is achieved by the resonance volume integrated in the compressor housing and the flow silencer in the high-pressure line. On the high pressure side, the frequencies of the further pressure pulsation peaks are also integer multiples of the rotational frequency and result from flow reflections. For frequencies greater than 400 Hz, the amplitude of the high-pressure pulsations drops at approx. 30 dB per decade.

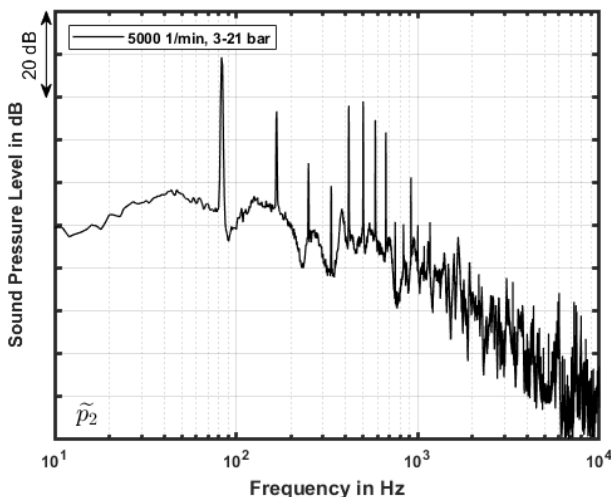


Figure 6. High pressure pulsation

3.2 Structure-borne sound

The investigated scroll compressor shows a complex vibration behaviour due to its large number of components and the different types of excitation. The vibration excitation is caused by forces from the eccentric movement of the orbiting compressor scroll, the rotation of the electric motor, the translational motion of the discharge valve as well as by pressure forces of the refrigerant flow.

Fig. 7 shows the vibration velocity level over the frequency from 10 to 10000 Hz. The signals of the three triaxial acceleration sensors at the bolting points have been quadratically averaged. Similar to the spectra of the pressure pulsations, the frequencies of the strongly pronounced tonal components are integer multiples of the rotational frequency. The amplitude of the velocity peaks depends on whether vibrational resonances are excited at the respective frequency. Basically, the first 2-3 orders are strongly pronounced in the range below 300 Hz and vibrations occur more strongly in the range from 700 to 2000 Hz.

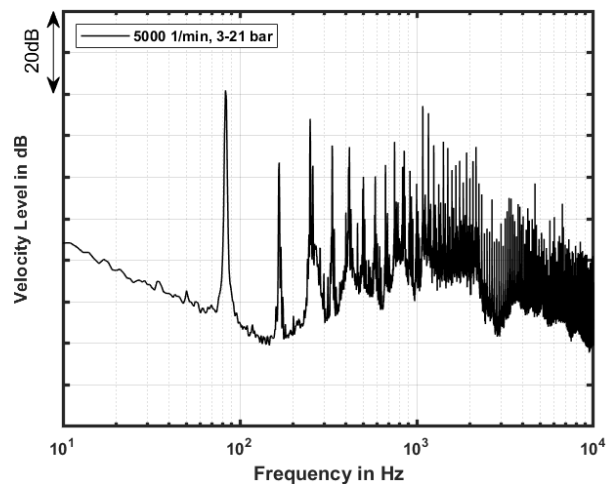


Figure 7. Vibrations at the bolting points

3.3 Airborne sound

Fig. 8 shows the sound pressure level over the frequency range from 10 to 10000 Hz, the signals of the 5 free-field microphones were quadratically averaged. The sound pressure level spectrum shows a multitude of peaks whose frequencies correspond to integer multiples of the rotational frequency. The spectrum of the radiated airborne

sound agrees well with the vibration spectrum (comp. Fig. 7). The maximum sound pressure level amplitude occurs at the 1st order and sound is emitted more strongly in the frequency range from 700 to 2000 Hz. This indicates that the radiated airborne sound mainly results from the vibrations of the compressor, this corresponds to findings of Lee et al. [6] and Miao et al. [7].

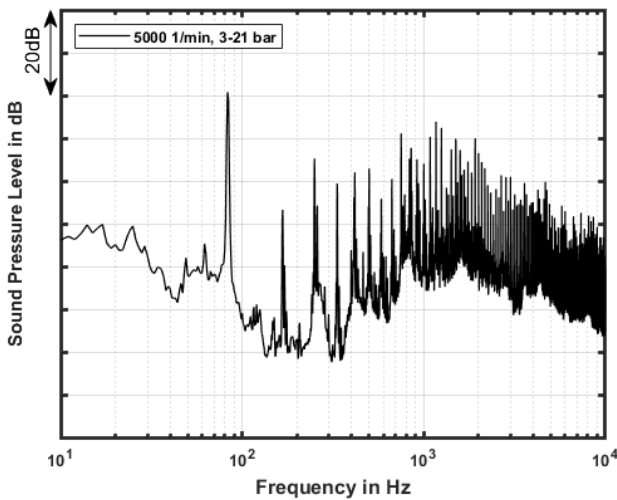


Figure 8. Radiated airborne sound

4. INFLUENCE OF THERMODYNAMIC PROCESS VARIABLES ON SCROLL COMPRESSOR ACOUSTICS

The aim of the investigations carried out is to determine the influence of speed, compression ratio, suction and high pressure on the acoustics of a scroll compressor. Measurements were carried out at low, medium and high compression ratio, once at constant suction pressure p_1 with corresponding adjustment of the high pressure p_2 and once at constant high pressure and corresponding adjustment of the suction pressure. The compression ratio ϵ is calculated according to formula 1:

$$\epsilon = \frac{p_2}{p_1} \quad (1)$$

The operating points investigated are listed in Tab. 1 and Tab. 2. In addition, each pressure ratio was measured at 3000, 5000 and 7000 rpm to be able to characterise the influence of low, medium and high speed. The measurements were carried out at constant speed, as the thermo-

dynamic boundary conditions such as pressures and superheat can be set more accurately at constant speed. The superheat of the refrigerant at the compressor inlet was set to 10 K for all measurements to ensure that only purely gaseous refrigerant enters the compression chamber.

Table 1. Operating points with constant suction pressure

Compression ratio ϵ [-]	5	7	9
Suction pressure p_1 [bar]	3	3	3
High pressure p_2 [bar]	15	21	27

Table 2. Operating points with constant high pressure

Compression ratio ϵ [-]	5	7	9
Suction pressure p_1 [bar]	4.2	3	2.33
High pressure p_2 [bar]	21	21	21

The pressure ratios listed in Tab. 1 and Tab. 2 were set by adjusting the heat flows to the condenser and evaporator and regulating the throttling effect of the expansion valve. At the same time, the position of the expansion valve influences the mass flow circulating in the refrigeration cycle. Fig. 9 shows the refrigerant mass flow as a function of the operating point, the values of the reference operating point at medium compression ratio are shown as black dots.

The mass flow increases proportionally to the pressure on the suction side, as this also increases the refrigerant mass entering the outer compression chambers. The mass flow increases linearly with the rotation speed due to the fixed volume of the screw geometry. For very high mass flow rates, the increment of the mass flow decreases as speed increases, due to the flow resistance in the refrigeration cycle increasing quadratically to the flow velocity. The compression ratio, on the other hand, has no measurable influence on the mass flow, since the quantity of refrigerant delivered remains the same at constant suction pressure and varying high pressure.

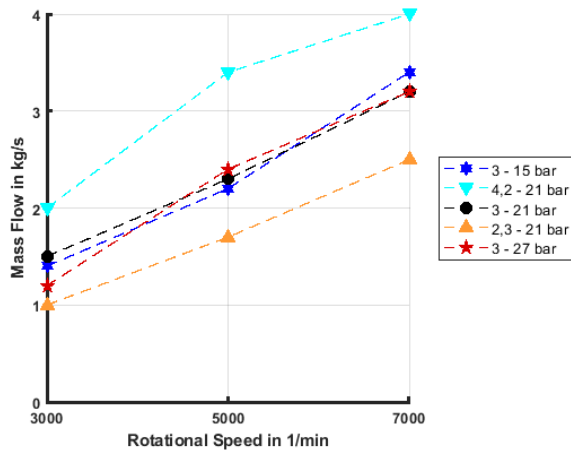


Figure 9. Refrigerant mass flow as a function of the operating point

4.1 Fluid sound

The values of the overall sound pressure level of the suction pressure pulsations for the different operating points are shown in Fig. 10. For the overall sound pressure level, the sound pressure level values were summed up over the frequency range of 10-10000 Hz. The pressure pulsations on the suction side increase with increasing speed and increasing suction pressure. The suction pressure pulsations are proportional to the delivered mass flow, recognisable by the strong correspondence with the mass flow shown in Fig. 9. Changes in high pressure and compression ratio have no effect on the pressure pulsations at the compressor inlet.

The pressure pulsations at the compressor outlet, on the other hand, show a different behaviour (see Fig. 11). Maximum values are shown at 3000 rpm since at low rotation speeds the individual compression pulses occur at greater intervals and thus merge less. At medium speeds, the high-pressure pulsations decrease and increase again at high speeds. In order to better explain this behaviour, the influence of the resonance volume integrated in the compression housing as well as the downstream flow silencer must be examined more closely. Increasing the high pressure and the compression ratio results in larger values of the overall sound pressure level of the high-pressure pulsations.

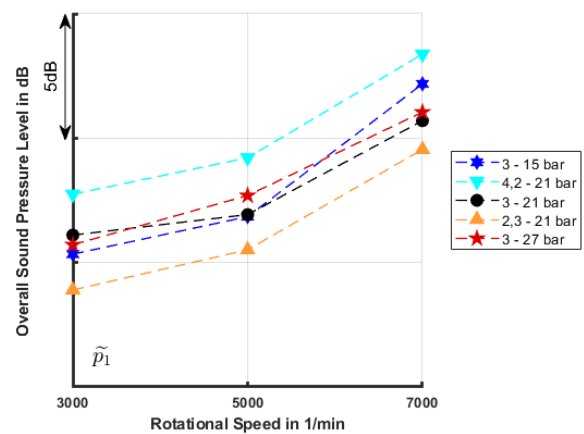


Figure 10. Suction pressure pulsations as a function of the operating point

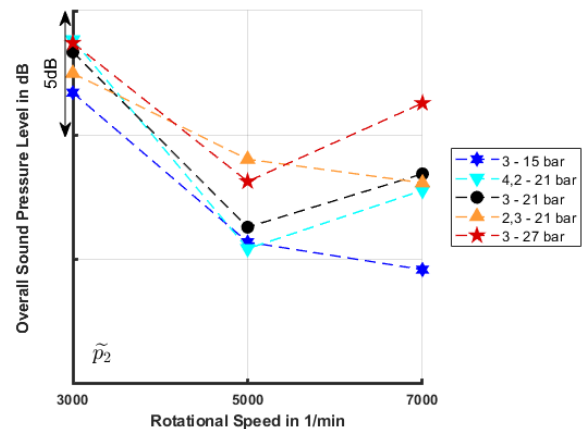


Figure 11. High pressure pulsations as a function of the operating point

4.2 Structure-borne sound

Fig. 12 shows the values of the overall vibration velocity level for the different operating points. For the overall velocity level, the velocity level values were summed up over the frequency range of 10-10000 Hz.

The vibration velocity of the compressor increases linearly with the speed. As high pressure and compression ratio increase, compressor vibrations increase slightly due to greater pressure forces in the compression chamber and at the outlet. At 7000 rpm an outlier appears, the maximum overall velocity level occurs at low compression ratio and low high pressure of 15 bar. The reason for this be-

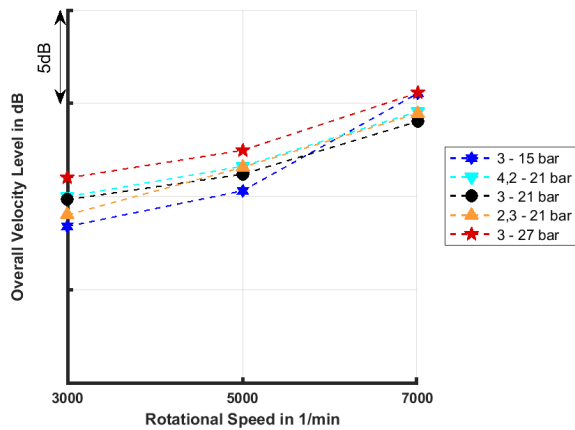


Figure 12. Vibrations at the bolting points as a function of the operating point

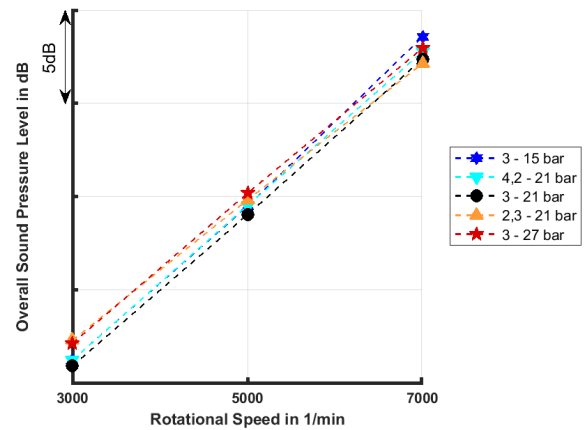


Figure 13. Airborne sound radiation as a function of the operating point

behaviour is still unclear, further investigations using a laser scanning vibrometer, are to be carried out on this.

The vibration behaviour of the compressor differs significantly from the value curves of the overall sound pressure level of the pressure pulsations on the suction side as well as on the high pressure side (comp. Fig. 10 and Fig. 11). Consequently, the influence of the pressure pulsations on the vibration excitation of the compressor is negligible.

4.3 Airborne sound

The overall sound pressure level values of the radiated airborne sound for the different operating points are shown in Fig. 13. For the overall sound pressure level, the sound pressure level values were summed over the frequency range 300-10000 Hz. The lower frequency was adjusted according to the acoustic properties of the anechoic room.

The sound pressure fluctuations radiated by the compressor increase linearly with speed, this corresponds to findings of Haeussler et al. [8]. Increasing high pressure and increasing compression ratio result in a small increment of the sound radiation. The value curve of the overall sound pressure level shows a high degree of agreement with the value curve of the overall velocity level at the attachment points (comp. Fig. 12). In contrast, the behaviour of the airborne sound radiation differs significantly from the value curves of the overall sound pressure level of the pressure pulsations on the suction side as well as on the high pressure side (comp. Fig. 10 and Fig. 11). From this it can be concluded that the radiated

airborne sound is mainly generated by the vibrating compressor surface. The influence of the refrigerant pressure pulsations on the sound radiation is negligible, a transmission of these pressure pulsations through the compressor housing does not occur.

5. SUMMARY

This paper describes the influence of the thermodynamic process variables speed, compression ratio as well as suction and high pressure on the acoustic properties of an electric refrigerant scroll compressor. For this purpose, different operating points were adjusted on a specially constructed refrigeration cycle test rig and fluid, structure-borne and airborne noise of the compressor were measured in an anechoic chamber.

The spectra of the investigated acoustic variables were evaluated for the reference measurement at medium speed and medium compression ratio. The spectra of fluid, structure-borne and airborne sound are dominated by a large number of narrow-band tonal components whose frequencies correspond to integer multiples of the compressor speed. In the refrigeration cycle, low-frequency pressure pulsations of the 1st and 2nd order are dominant. The spectra of vibrations and airborne sound show a high degree of correlation, vibrations and sound radiation are strongly pronounced in the higher frequency range from 700 to 2000 Hz.

The pressure pulsations on the suction side increase with raising suction pressure and increasing speed, they

are proportional to the refrigerant mass flow. The overall sound pressure level of the high pressure pulsations is particularly high at low rotation speeds. Vibrations and airborne sound radiation increase linearly with increasing speed. Compression ratio and pressure on the suction and the high-pressure side have only a minor influence on the vibration behaviour and sound radiation of the scroll compressor. The pressure pulsations and the mass flow in the refrigeration cycle and have no measurable influence on the vibroacoustic noise generation in the compressor. Since it was found that the speed is the dominant factor for scroll compressor acoustics, further investigations shall be performed over the complete speed range. Structure-borne and airborne noise are proportional to the speed, therefore low compressor speeds are desirable, especially in quiet driving conditions.

6. ACKNOWLEDGMENTS

The authors want to thank the AUDI AG for funding this research within the framework of the INI.FAU cooperation and supporting it with measurement equipment and know-how, most notably M. Kronbichler, Dr. C. Rebinger and S. Rost.

7. REFERENCES

- [1] EU Environment Council, "Fit for 55: Council adopts regulation on co2 emissions for new cars and vans," 2023.
- [2] J. Aurich and R. Baumgart, "Comparison and evaluation of different a/c compressor concepts for electric vehicles," in *Proc. of the International Compressor Engineering Conference*, vol. 2608, pp. 1434–1443, 2018.
- [3] A. Hofacker, "Akustik für fahrzeuge mit elektrifiziertem antrieb," *ATZ - Automobiltechnische Zeitschrift*, vol. 117, pp. 8–13, 2015.
- [4] A. Ricci, L. Bregant, and F. Albertz, "On the different contributions of flexible elements to the structural noise of refrigeration compressors," in *12th International Styrian Noise, Vibration and Harshness Congress: The European Automotive Noise Conference*, vol. 694, pp. 504–508, 2022.
- [5] C. Wang, Z. Wang, W. Yan, H. Li, and C. Yangi, "Study on characteristics of the vibration and noise of high-power scroll compressor," *Shock and Vibration*, vol. 2021, pp. 1–17, 2021.
- [6] J.-K. Lee, S.-J. Lee, and D.-S. Lee, "Identification and reduction of noise in a scroll compressor," in *Proc. of the International Compressor Engineering Conference*, vol. 1496, pp. 1041–1048, 2000.
- [7] Q. Miao, Y. R. Men, J. X. Wu, and X. Gou, "Studies on scroll compressor noise improvement," in *Engineering and Technological Solutions for Sustainable Development*, vol. 694, pp. 504–508, 2014.
- [8] M. Haeussler, D. Kobus, and D. Rixen, "Parametric design optimization of e-compressor nvh using blocked forces and substructuring," *Mechanical Systems and Signal Processing*, vol. 150, 2020.
- [9] M. Yanasigawa, T. Uematsu, S. Hiodoshi, M. Saito, and S. Era, "Noise reduction technology for inverter controlled scroll compressors," in *Proc. of the International Compressor Engineering Conference*, vol. 1578, 2002.